Measurements of Electron Density and Temperature in a Miniature Microwave Discharge Ion Thruster using Laser Thomson Scattering Technique

Yamamoto, Naoji
Department of Advanced Energy Engineering Science, Kyushu University

Tomita, Kentaro
Department of Applied Science for Electronics and Materials, Kyushu University

Yamasaki, Naoto
Department of Applied Science for Electronics and Materials, Kyushu University

Tsuru, Teppei
Department of Advanced Energy Engineering Science, Kyushu University

他

Measurements of Electron Density and Temperature in a Miniature Microwave Discharge Ion Thruster using Laser Thomson Scattering Technique

N Yamamoto[1], K Tomita[2], N Yamasaki[2], T Tsuru[1], T Ezaki[1], Y Kotani[1], K Uchino[2] and H Nakashima[1]

[1]*Department of Advanced Energy Engineering Science, Kyushu University*
6-1 Kasuga-kouen, Kasuga, Fukuoka 816-8580, Japan
[2]*Department of Applied Science for Electronics and Materials, Kyushu University,*
6-1 Kasuga-kouen, Kasuga, Fukuoka 816-8580, Japan

Corresponding author: yamamoto@aees.kyushu-u.ac.jp

Keywords: Ion thruster, Laser Thomson scattering technique, Electric propulsion.

Abstract. In order to improve the thrust performance of a miniature microwave discharge ion thruster, the relationship between electron number density/temperature and operational conditions, mass flow rate, incident microwave power and magnetic field strength were measured by means of laser Thomson scattering. A photon counting method and a triple grating spectrometer were used against a small Thomson scattering signal and a strong stray laser light. Electron number density increased with incident microwave power and was saturated at critical incident microwave power; it was about 1.2×10^{18} m^{-3} at incident microwave power > 8 W. In addition, electron number density increased with mass flow rate and became saturated; it was about 1.7×10^{18} m^{-3} at mass flow rate > 0.04 mg/s. The electron number density gradually increased with an increase in the number of magnets, i.e., magnetic field strength. There was a sudden jump at thirteen magnets, although the thruster failed to ignite at fourteen magnets. This is because there is an optimum distance between the antenna and the electron cyclotron resonance layer. These results suggest that future improvement in thrust efficiency in miniature microwave discharge ion thrusters may come from the fine adjustment of the magnetic field configuration inside the discharge chamber.

1.   Introduction

The demand for mN class miniature propulsion systems for small satellites is expected to grow in the future [1], due to their relatively low cost and short development time, among other reasons [2-4]. Until recently, size restrictions have limited the capacity of the available propulsion systems, and this has restricted the capability of small satellites.   One of the candidates for mN class miniature propulsion systems is a miniature ion thruster, since an ion thruster produces high thrust efficiency (over 50%) with a specific impulse of 3,000-8,000 sec [5-7].

Several studies have been conducted on the miniature ion thruster [8-11]. Wirz showed good performance of a 30 mm Miniature Xenon Ion (MiXI) thruster[8], that is, the thrust and the thrust efficiency were 1.5 mN and 0.56, for 43 W of input power and 0.05 mg/s of mass flow rate, $\dot{m}$. An electron bombardment-type ion source was used for ion production, so that operation time was limited by the thermionic cathode lifetime. A microwave discharge ion source would offer a potentially longer thruster lifetime than the electron bombardment-type, since it would be free from contamination and degradation of electron emission capacity [9, 10].

Therefore, we have developed a miniature microwave discharge ion thruster. The thrust performance of our ion thruster, that is, thrust and thrust efficiency, are 0.79 mN and 0.57, respectively at xenon $\dot{m}$ = 0.018 mg/s and input power of 28 W (incident microwave power, P_i, of 8 W). This performance is competitive with that of the thruster developed by Wirz, which has hither to shown the best performance in this class of miniature thruster. In addition, for P_i=16 W, xenon $\dot{m}$ =0.036 mg/s and beam voltage of 1,500 V, the ion beam current density in the vicinity of the grids for the previous condition is 120 A/m^2, which is about four times larger than that of the ion engine developed at NASA [6]. Thus, the plasma density in the discharge chamber would be higher, which is a great advantage for

2

application to small satellites. For practical applications, some improvement in the thrust performance will still be required.

In order to understand the physics in the discharge chamber and to design an appropriate grid system, investigation of the relationship between electron number density, N_e, and electron energy distribution function (EEDF) (electron temperature, T_e) in the discharge chamber and thruster operational configuration is essential. Furthermore, this information will play an important role in the validation of the numerical models for estimation of the life expectancy of the ion thruster [12]. Until now, however, the plasma properties inside the miniature ion thruster have been measured primarily by means of intrusive methods, such as electrostatic probes, which tend to disturb the plasma.

Therefore, the aim of this study is to investigate the dependency of plasma properties in the discharge chamber on operational conditions, incident microwave power, mass flow rate and magnetic field strength by laser Thomson scattering (LTS). LTS is an optical method for a measurement of plasma properties. So the perturbation by this method is little in comparison with an electrostatic probe method. In the incoherent regime, the scattered spectrum reflects the Doppler motion of individual electrons, and the scattered intensity is proportional to N_e. This method was developed to measure plasma properties in high temperature plasma having $N_e > 10^{19}$ m^{-3} [13-16]. During the last decade, its applicability has been extended to lower density plasma, with densities of less than 10^{16} m^{-3}, by a signal accumulation technique [14]. This technique allows us to apply LTS to the plasma produced in the miniature microwave ion thruster.

2. Experimental equipment

2.1. Microwave discharge ion thruster

The cross section of a 30 W class miniature microwave discharge ion thruster is shown in figure 1. The inner diameter is 21 mm and the size of the thruster is 50 mm×50 mm×30 mm. The ion source consists of an antenna and a magnetic circuit, which is made up of several samarium cobalt (Sm-Co) permanent magnets and iron yokes. The magnetic field strength inside the discharge chamber can be changed by changing the number of the permanent magnets, N_{mag}. The magnetic mirrors are located at the tip of a front yoke and the tip of a central yoke, as shown in figure.2. Microwave power at 2.45 GHz is fed through a coaxial line and into the antenna. A star antenna is used, since it showed good performance in previous studies [10, 17]. The antenna is inscribed in a 9 mm diameter circle and is made of molybdenum. The thickness of the antenna is 1 mm.

In this study, the ion beam was not extracted. Instead of grids, an orifice (ϕ=8 mm) is used in order to produce almost the same pressure as in the case of ion beam extraction from the plasma, assuming propellant utilization of 0.7 and a ratio of the doubly charged ion current to the singly charged ion current of 0.15; the conductance of the orifice is about three times larger than that of the grids. For the LTS measurements, krypton, rather than xenon, is used as a working gas. A previous study showed that the laser induced some perturbation on the xenon plasma [18]. This is due to photo-ionization of excited xenon atoms; xenon atoms at the excited state are ionized by the laser (wavelength 532 nm and photon energy 2.3 eV), while no effect is observed for krypton plasma. Though the thrust performance using krypton gas is 20% inferior to the thrust performance using xenon gas[19], krypton is less expensive than xenon, so it is suitable for the application to low cost small satellites. In addition, the results obtained with krypton plasma shows the physics inside the discharge chamber, and this will contribute the improvement of the thrust performance with xenon; the

understanding of the physics tells us the optimum conditions, such as magnetic field strength and mass flow rate and among other factors.

A thermal mass flow controller was used. The flow rate error is less than 5% for most of the conditions. A 0.3 m diameter by 0.4 m long vacuum chamber was used in the experiments. The pumping system comprised a turbo molecular pump. The background pressure was maintained below 5.0×10^{-2} Pa for most of the operating conditions.

2.2. Thomson scattering measurement system

Figure 3 shows the experimental setup for LTS measurements on the miniature microwave discharge ion thruster. The scattering light inside the discharge chamber is collected through a hole (ϕ=3 mm) and the laser beam go pass through two small holes (ϕ= 2 mm). The ϕ= 3 mm hole is positioned at an angle of 90 degree to the laser pass.

The light source is the second harmonic beam of an Nd:YAG laser having a wavelength of 532 nm with an energy of 180 mJ, a repetition rate of 10 Hz, a pulse width of 6 ns and a beam divergence of 0.6 mrad. The measurement points are 4 mm downstream of the antenna on the *z* axis. One is on the thruster axis and the other is 6 mm off the axis, as shown in figure. 3. The laser beam is focused at a distance of 4 mm from the tip of the microwave discharge antenna through a focusing lens (*f*=300 mm). The size of the focal spot was estimated as 0.08 mm in diameter, by observing the spatial profile of Rayleigh scattering from 40 kPa air gas. Scattered light from the plasma is focused onto the entrance slit of the triple grating spectrometer (TGS) with two achromatic lenses of $f = 350$ mm and $f = 250$ mm. The scattering volume is $0.08 \times 0.08 \times 1$ mm^3, as determined by the laser beam size, the slit width and the slit height, respectively. The solid angle of observation is about 0.025 sr. Strong stray light is generated

from the surface of the components, due to the small size of discharge chamber, and the LTS signals are overwhelmed by it. In order to reduce stray light, the discharge chamber wall was made of carbon and TGS was used. The scattered light is dispersed by passing through the TGS, and is detected by a photomultiplier tube (PMT). The TGS used in this experiment could reduce stray light around 10^{-8} at the wavelength of 2 nm from the probing laser, where the LTS signal is observed.

The estimated Thomson scattered photon number is so small that we used a photon counting method. The detected Thomson scattered signals were analyzed by a photon counter after more than 5000 laser shots had been accumulated. The data accumulation process technique, taking advantage of the DC or repetitive operation of some discharges, was first suggested for lowering the limiting electron densities by Sakoda et al. [20]. We count photons for three conditions at each wavelength, condition 1; with plasma and laser, condition 2; plasma without laser, and condition 3; laser without plasma. We evaluate actual LTS signal by subtracting the number of photons obtained for condition 2 and 3 from the number of photons obtained for condition 1.

3.   Results and Discussion

Figure 4 shows LTS signal count number per 5000 laser shots on a logarithmic scale against $(\Delta\lambda)^2$ at krypton $\dot{m}$ =0.025 mg/s, and P_i= 16 W, where $\Delta\lambda$ is the difference between the laser wavelength (532 nm) and the measured wavelength. $(\Delta\lambda)^2$ is proportional to the electron energy; the signal at $(\Delta\lambda)^2 = 2.2$ nm^2 corresponds to scattering from the electrons with an energy of 1 eV. Thus, we observed electrons at energy levels between 2 to 5.6 eV, since $\Delta\lambda$ is from 1.5 nm to 3.5 nm in this experiment. The statistical uncertainty of the LTS measurements is determined by the shot noise of the

detected number of photons [15]. The observed electron energy distribution function is Maxwellian, since the scattered spectrum can be fitted by a Gaussian at a temperature of 5.2 eV. From this spectrum and the Rayleigh scattering calibration using air, electron number density is estimated as $9.8 \pm 2.0 \times 10^{17}$ m^{-3} (where the error is due to the shot noise).

Figures 5 and 6 show the dependence of N_e and T_e on $\dot{m}$ for two positions, on-axis and off-axis. T_e at $\dot{m}$ =0.012 mg/s at the on-axis and off-axis positions is 8.6 eV and 7.0 eV, respectively. We see the same tendency as above in all the mass flow rates tested. That is, T_e at off-axis is higher than at on-axis. This can be explained as follows. Trapped electrons gain energy from the microwaves when they go through the electron cyclotron resonance (ECR) layer while bouncing between magnetic mirrors, as shown in figure. 2. Thus, electrons at the off-axis position are energized by the microwaves several times, since they go through the ECR layer several times, since they go through the ECR layer several times, until they finally lose energy by collision with neutral atoms; approximate mean free path is about 0.4 m, therefore, electrons pass through the ECR layer about 30 times. Electrons on-axis positions gain little energy from the microwaves since electric field deduced by the antenna is parallel to the magnetic field as shown in Fig7 and, therefore, does not contribute to the ECR heating of on-axis electrons.

With an increase in $\dot{m}$, T_e is decreased for both positions, that is, 8.6 eV at $\dot{m}$ =0.012 mg/s and 4.6 eV at $\dot{m}$ =0.05 mg/s at off-axis and 7.0 eV at $\dot{m}$ =0.012 mg/s and 3.2 eV at $\dot{m}$ =0.05 mg/s at the on-axis position. This is because the mean free path of the electrons is shortened with an increase in $\dot{m}$, that is, an increase in pressure inside the discharge chamber. This leads to a reduction in the chance that electrons will go through the ECR layer while bouncing back and forth between the magnetic

mirrors. This means that electrons recieve less energy from the microwaves and this leads to the decrease in T_e.

N_e at the on-axis position is higher than that at the off-axis position for all mass flow rates; $1.6\pm0.3\times10^{18}$ m^{-3} on-axis position, and $0.82\pm0.16\times10^{17}$ m^{-3} off-axis for $\dot{m}$ =0.012 mg/s. These results show that the loss of plasma is primarily due to the recombination on the wall and the antenna surface, not in the whole volume of the discharge chamber, and that ionization is occurring in the whole volume of the discharge chamber. That is, the high energy electrons gained by microwaves would diffuse to the whole of the discharge chamber and ionize neutral atoms. Therefore, N_e at the on-axis position, that is, the furthest position from the wall, is larger than that at the off-axis position, even if T_e is smaller, since the influence of the loss on the walls is small.

With an increase in $\dot{m}$, N_e at both positions increases; N_e at the on-axis position for $\dot{m}$ =0.025 mg/s, $\dot{m}$ =0.037 mg/s and $\dot{m}$ =0.05 mg/s is $1.2\pm0.2\times10^{18}$ m^{-3}, $1.7\pm0.3\times10^{18}$ m^{-3} and $1.8\pm0.4\times10^{18}$ m^{-3}, respectively. This is due to the increase in the number density of neutral atoms in the discharge chamber and increasing ionization. The exception is the condition at the on-axis position for $\dot{m}$ = 0.012 mg/s. In this condition, high energy electrons diffuse from off-axis position and this leads to an increase in the chance of ionization, even if the pressure is low. On the other hand, at off-axis position, the effect of an increase in the ionization rate is canceled by the effect of an increase in diffusion rate, therefore, the number density at $\dot{m}$ =0.012 mg/s is smaller than that at $\dot{m}$ =0.025 mg/s.

Figure 8 shows the relation between plasma property and incident microwave power at $\dot{m}$ =0.025 mg/s for the off-axis position. N_e for P_i=4 W, 8 W, 12 W and 16 W is $0.6\pm0.1\times10^{18}$ m^{-3}, $1.2\pm0.2\times10^{18}$ m^{-3}, $1.1\pm0.2\times10^{18}$ m^{-3} and $1.0\pm0.2\times10^{18}$ m^{-3}, respectively. T_e for P_i=4 W, 8 W, 12 W and 16 W is 3.9 eV, 5.0 eV, 5.2 eV and 5.2 eV, respectively. That is, with an increase in P_i, N_e and T_e are increased but

saturated beyond critical microwave power, in this case, 8 W. This means that too much incident microwave power results in an increase in loss. This does not contribute to the improvement of thrust efficiency, since thrust efficiency of ion thrusters, η_t, can be expressed as[21],

$$\eta_t = \frac{\gamma_T^2}{1+(P_i)/(I_b \times V_b)} \frac{I_b}{(e/M_i)\cdot(\dot{m})} \tag{1}$$

where γ_T, I_b, P_i, V_b, e, M_i, $\dot{m}$ are thrust coefficient, extracted ion beam current, incident microwave power, beam voltage, electronic charge, ion mass and mass flow rate, respectively.

Considering the exhaust-beam divergence and the effect of doubly charged ion, γ_T is defined as

$$\gamma_T = \cos\theta_b \times \left(1+\alpha/\sqrt{2}\right)/(1+\alpha) \tag{2}$$

where θ_b, and α are beam divergence angle and the ratio of doubly charged ion current to singly charged ion current, respectively. α and θ_b are assumed to be 0.15 and 10 degrees [22, 23], respectively. Thus, in this study, γ_T is estimated as $\gamma_T \approx 0.98 \cdot 0.96 = 0.94$.

According to the Bohm sheath criterion, the velocity of an ion from the plasma into the ion sheath on a grid is assumed to be Bohm velocity, V_B, expressed as follows.

$$V_B = \sqrt{\frac{kT_e}{M_i}} \tag{3}$$

where k and T_e are Boltzmann constant and electron temperature, respectively. Given that n_e in the bulk plasma decreases by a factor of exp (-1/2) at the point where the ion velocity reaches V_B, the ion beam current is evaluated as below.

$$I_b = en_e \, exp\left(-\frac{1}{2}\right) S \sqrt{\frac{kT_e}{M_i}} \tag{4}$$

where S is total ion beam extraction area.

That is, if the incident microwave power is constant, higher plasma density or electron temperature will provide better thrust efficiency, and vice versa.

Figure 9 shows the dependence of plasma properties on magnetic field strength at $\dot{m}$ =0.025 mg/s

for the off-axis position. The magnetic field strength inside the discharge chamber was changed by

changing N_{mag}. N_e and T_e are almost constant while $N_{mag} \leq 12$, and suddenly jump at N_{mag} =13. Figure

10 shows the magnetic field profile for various numbers of magnets (calculated using QuickField 3.4

[24], Tera Analysis Co.). The antenna does not overlap the ECR layer at N_{mag} =13, as shown in

figure.10, while it does overlap the ECR layer at $N_{mag} \leq 12$; this would lead to a decrease in loss on

the antenna, and leads to an increase in N_e and T_e. When N_{mag} =14, the plasma was not ignited. This is

because the ECR layer at N_{mag} =14 is too far away from the antenna, which generates an electric field

on the ECR layer. In addition, the magnetic field vector at the ECR layer is almost parallel to the

electric field generated by the antenna, as shown in Fig. 7. Thus, the electric field perpendicular to the

magnetic field (which contributes to the acceleration of electrons) is too small to ignite the plasma.

Therefore, the plasma was not ignited at N_{mag} =14.

4. Summary

LTS should contribute to the improvement of electric propulsion systems, ion thrusters, Hall

thrusters, and other thrusters, as a powerful tool for understanding the physics of these systems. The

demonstrated LTS measurements probed the plasma properties of a 30 W class miniature microwave

discharge ion thruster; we have investigated the dependence of plasma properties on mass flow rate,

incident microwave power, and number of permanent magnets. These results show the direction for

the improvement of the thrust efficiency in the miniature microwave discharge ion thruster. That is, we

found that the electron temperature is inversely proportional to the mass flow rate. Electron number

density first decreases with an increase in mass flow rate beyond critical mass flow rate and then increases with a further increase in mass flow rate. Thus, ion thrusters should be operated below this critical mass flow rate. Number density and electron temperature are saturated beyond critical incident microwave power; therefore, we should operate below this critical incident power for optimal thrust performance. There is also an optimal magnetic field configuration; in this case, the number of magnets is thirteen. Magnetic field analysis confirms the antenna and the ECR layer should not be overlapped, but they should be close.

References:

[1] Mueller J 2000 Thruster Options for Microspacecraft: A Review and Evaluation of State-of-the Art and Emerging Technologies, *Micropropulsion for Small Spacecraft*, ed Micci M M and Ketsdever A D *Progress in Astronautics and Aeronautics* vol. **45**, (Reston, VA:AIAA) pp 45–137

[2] Kato M, Takayama S, Nakamura U, Yoshihara K. and Hashimoto H, 2005 IAC Paper 05.B5.6.B.01

[3] Barnhart D, Vladimirova T and Sweeting M, 2007 *J. of Spacecraft and Rockets* **44** 1294.

[4] Muller J, Marrese C, Polk J, Yang E, Green A, White V, Bame D, Chadraborty I and Vargo S 2003 *Acta Astronautica* **52** 881.

[5] Wilbur P J, Rawlin V K and Beattie J R 1998 *J. Propul. Powe,* **14** 708

[6] Sovey J S, Rawlin V K and Patterson M J 2001 *J. Propul. Power* **17** 517

[7] Funaki I, Kuninaka H and Toki K 2004 *J. Propul. Power* **20** 718

[8] Wirz R E, Ph. D. Diss. 2005 California Institute of Technology

[9]   Nakayama Y, Funaki I, and Kuninaka H 2007 *J. Propul. Power* **23** 495

[10] Yamamoto N, Masui H, Kataharada H, Nakashima H and Takao Y 2006 *J . Propul. Power* **22** 925

[11] Tsay M M, 2006 Master Thesis, Massachusetts Institute of Technology

[12] Nakano M, Tachibana T and Arakawa Y, 2002 *Trans. of the Jap. Soc. for Aero. and Space Sciences* .**45** 154

[13] Evans D E and Katzenstein J 1969 *J. Rep. Prog. Phys.* **32** 207

[14] Muraoka K, Uchino K and Bowden M D,1998 *Plasma Phys. Controlled Fusion* **40** 1221.

[15] Kunze H J, 1968 The laser as a tool for plasma diagnostic, *Plasma diagnostics*, ed. Lochte-Holtgreven W, (Amsterdam: Noth-Holland Publishing Company) 550

[16]   DeSelva A W and Goldenbaum G C 1970 Plasma diagnostics by light scattering *Methods of Experimental Physics*, vol. **9** *Plasma Physics* A ed. Griem H R and Lovberg R H (New York: Academic Press) pp.61-113.

[17] Yamamoto N, Kondo S, Chikaoka T and Nakashima H, 2007 *J. Appl. Phys.,* **102***,* 123304

[18] Kim Y K, Tomita K, Hassaballa S, Uchino K, Muraoka K, Hatanaka H, Kim Y M, Lee S E, Son S H and Jang S H 2004 SID International Symposium Digest of Technical Papers, **35**, 550

[19] Yamamoto N, Miyoshi M, Takao Y and Nakashima H, 2002 *Trans. of the Jap. Soc. for Aero. and Space Sciences* .**7** pb_119

[20] Sakoda T, Momii S, Uchino K, Muraoka K., Bowden M, Maeda,   M, Manabe, Y, Kitagawa, M, and Kimura, T 1991 *Jpn. J. Appl. Phys.* **30** L1425

[21] Brophy J R, Garner C E and Mikes S 2009 *J. Propul. Power* **25** 1189

[22] Satori S, Kuninaka H, and Otaki M 1998 *Jap. Soc. for Aero. and Space Sciences* **46** 406 (in Japanese).

[23]   Takegahara H, Kasai Y Gotoh Y, Miyazaki K, Hayakawa Y, Kitamura S, Nagano H, and Nanamura K, 1993 IEPC Paper 93-235, Electric Rocket Propulsion Society

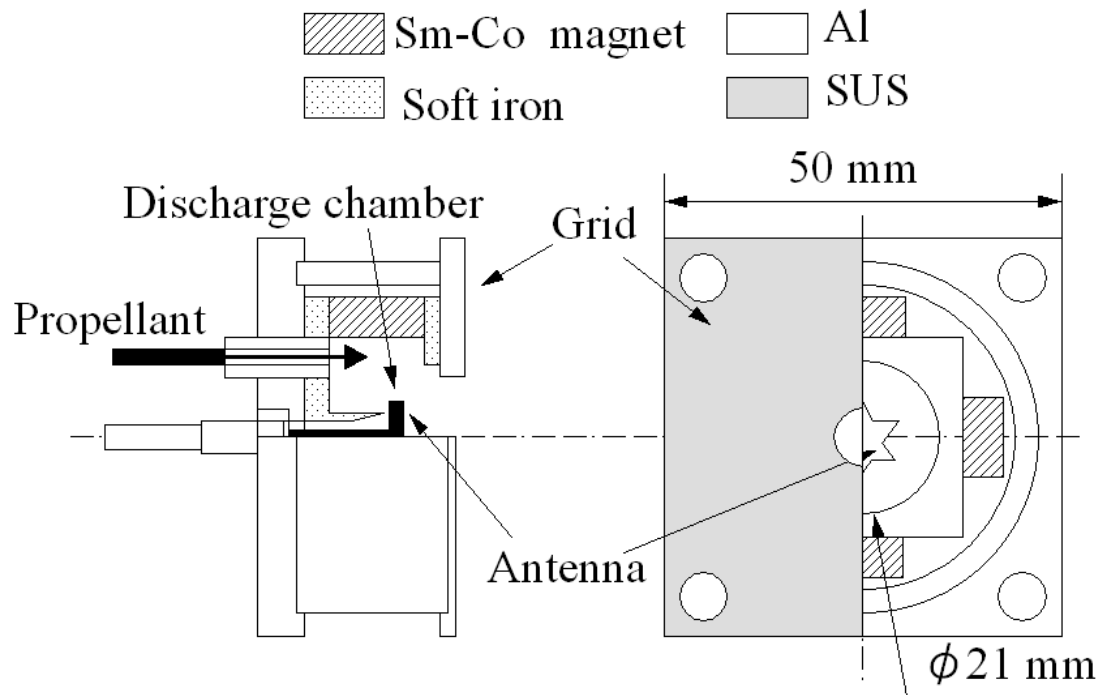[24] http://www.quickfield.com/

Figure Captions

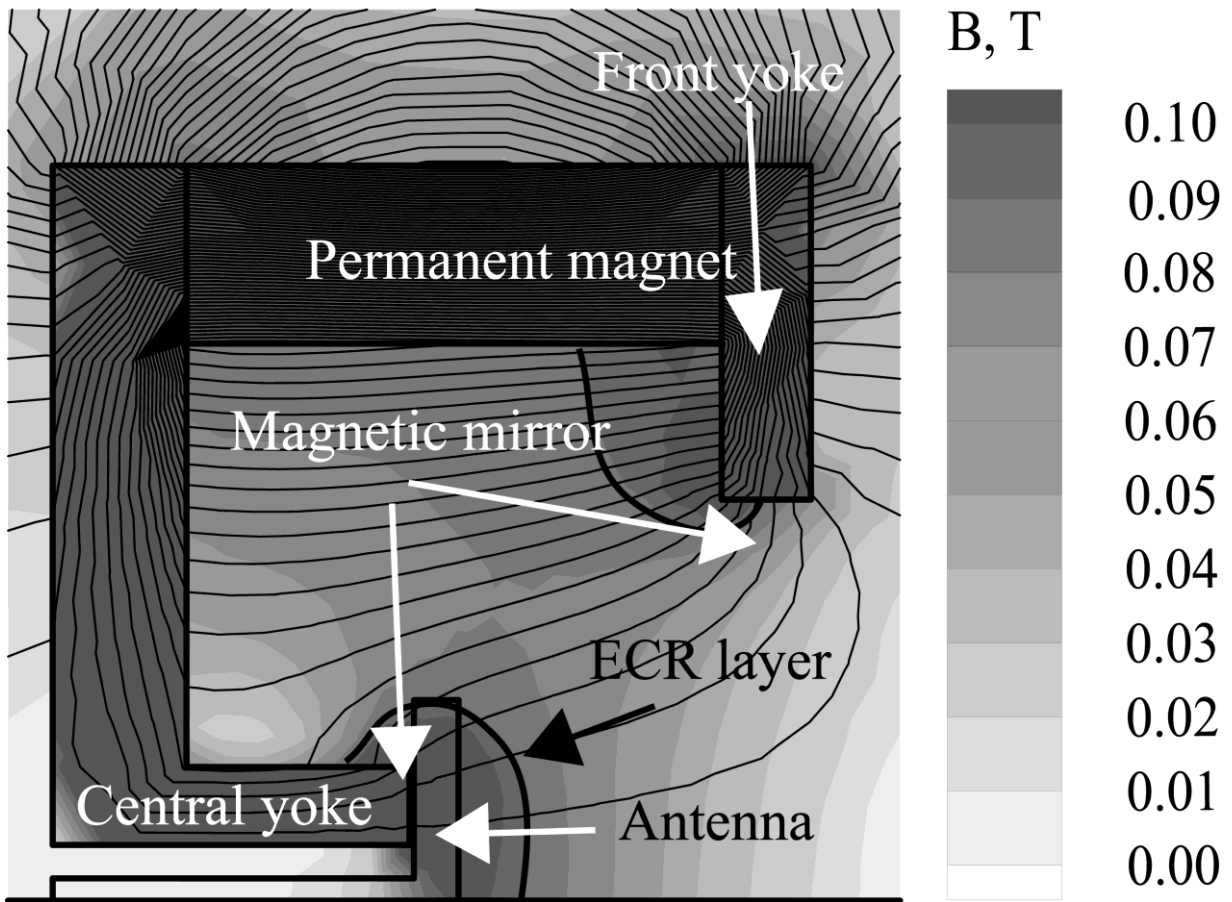Figure 1. Cross section of a miniature microwave discharge ion thruster developed at Kyushu University.

Figure 2. Magnetic field profile of a miniature microwave discharge ion thruster developed at Kyushu University, with twelve magnets.
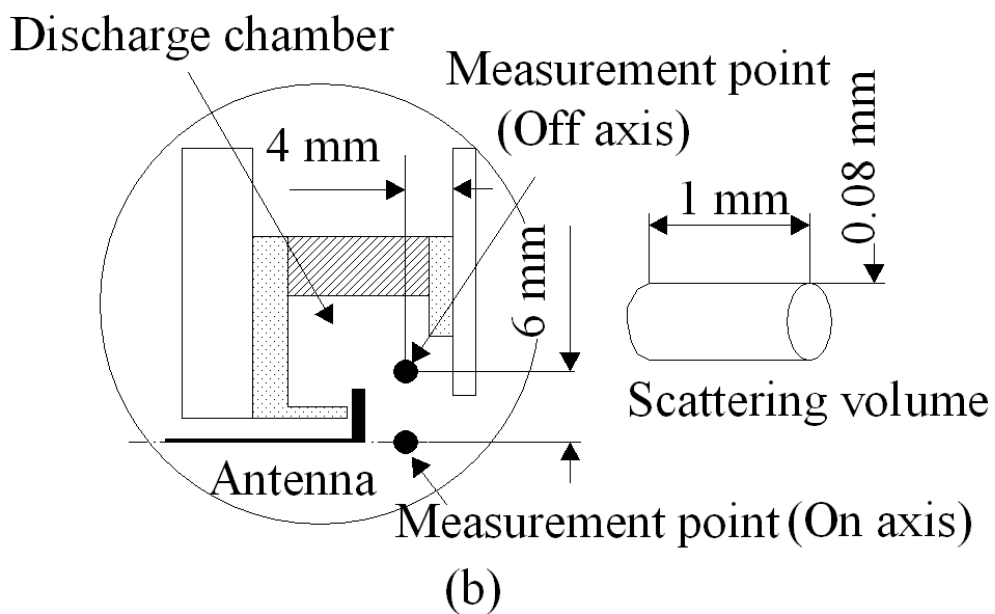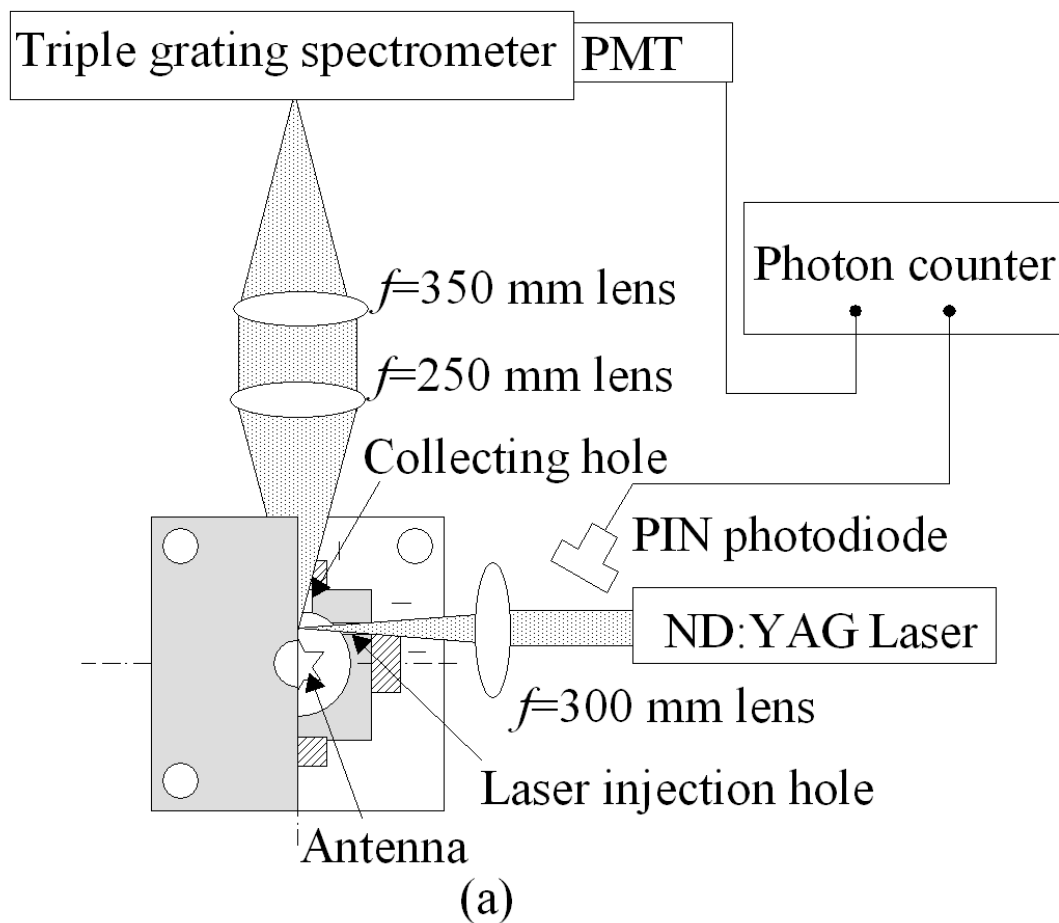
Figure 3 Experimental setup of LTS measurements on the miniature microwave discharge ion thruster. (a) front view (b) side view.
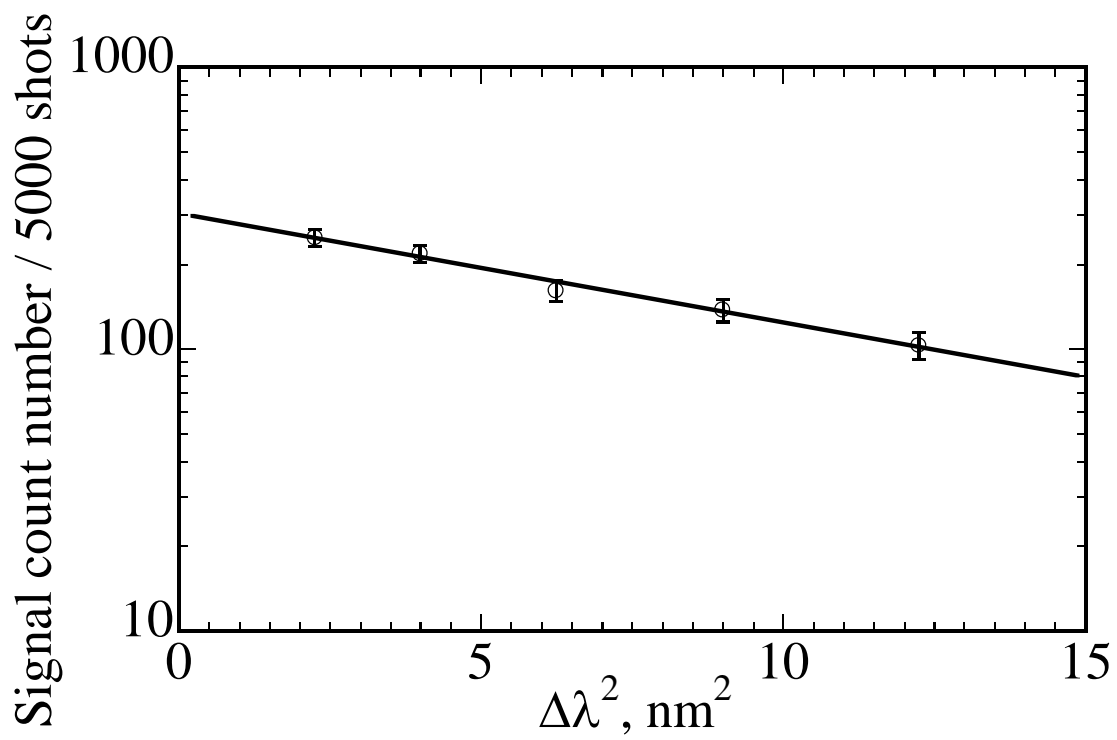
Figure 4. Thomson scattering spectrum at krypton mass flow rate of 0.025 mg/s, and incident microwave power of 16 W with twelve magnets.
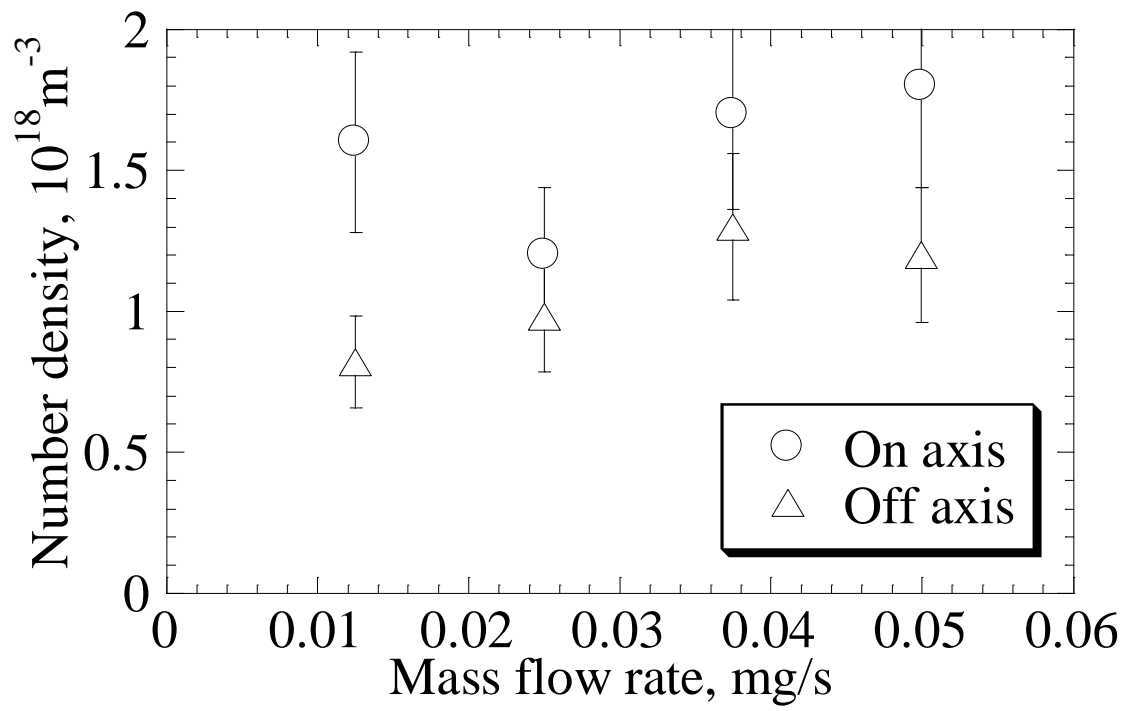
Figure 5. Dependence of plasma density on mass flow rate for two positions at incident microwave power of 16 W with twelve magnets.

Figure 6. Dependence of electron temperature on mass flow rate for two positions at incident microwave power of 16 W with twelve magnets.

Figure 7. Electric field profile of a miniature microwave discharge ion thruster developed at Kyushu University, .

Figure 8. Dependence of plasma properties on incident microwave power at krypton mass flow rate of 0.025 mg/s, with twelve magnets.

Figure 9. Dependence of plasma properties on the number of magnets at krypton mass flow rate of 0.025 mg/s and incident microwave power of 16 W.

Figure 10. Magnetic field profile for various numbers of magnets, (a) N_{mag} = 10, (b) N_{mag} = 12, (c) N_{mag} = 13, (d) N_{mag} = 14.

Figure 1. Cross section of a miniature microwave discharge ion thruster developed at Kyushu University.

Figure 2. Magnetic field profile of a miniature microwave discharge ion thruster developed at Kyushu

University, with twelve magnets.

Triple grating spectrometer PMT

Photon counter

f=350 mm lens

f=250 mm lens

Collecting hole

PIN photodiode

ND:YAG Laser

f=300 mm lens

Laser injection hole

Antenna

(a)

Discharge chamber

Measurement point
(Off axis)

4 mm

0.08 mm

6 mm

1 mm

Scattering volume

Antenna

Measurement point (On axis)

(b)

Figure 3. Experimental setup of LTS measurements on the miniature microwave discharge ion thruster.

(a) front view (b) side view.

Figure 4. Thomson scattering spectrum at krypton mass flow rate of 0.025 mg/s, and incident microwave power of 16 W with twelve magnets.

Figure 5. Dependence of plasma density on mass flow rate for two positions at incident microwave

power of 16 W with twelve magnets.

Figure 6. Dependence of electron temperature on mass flow rate for two positions at incident
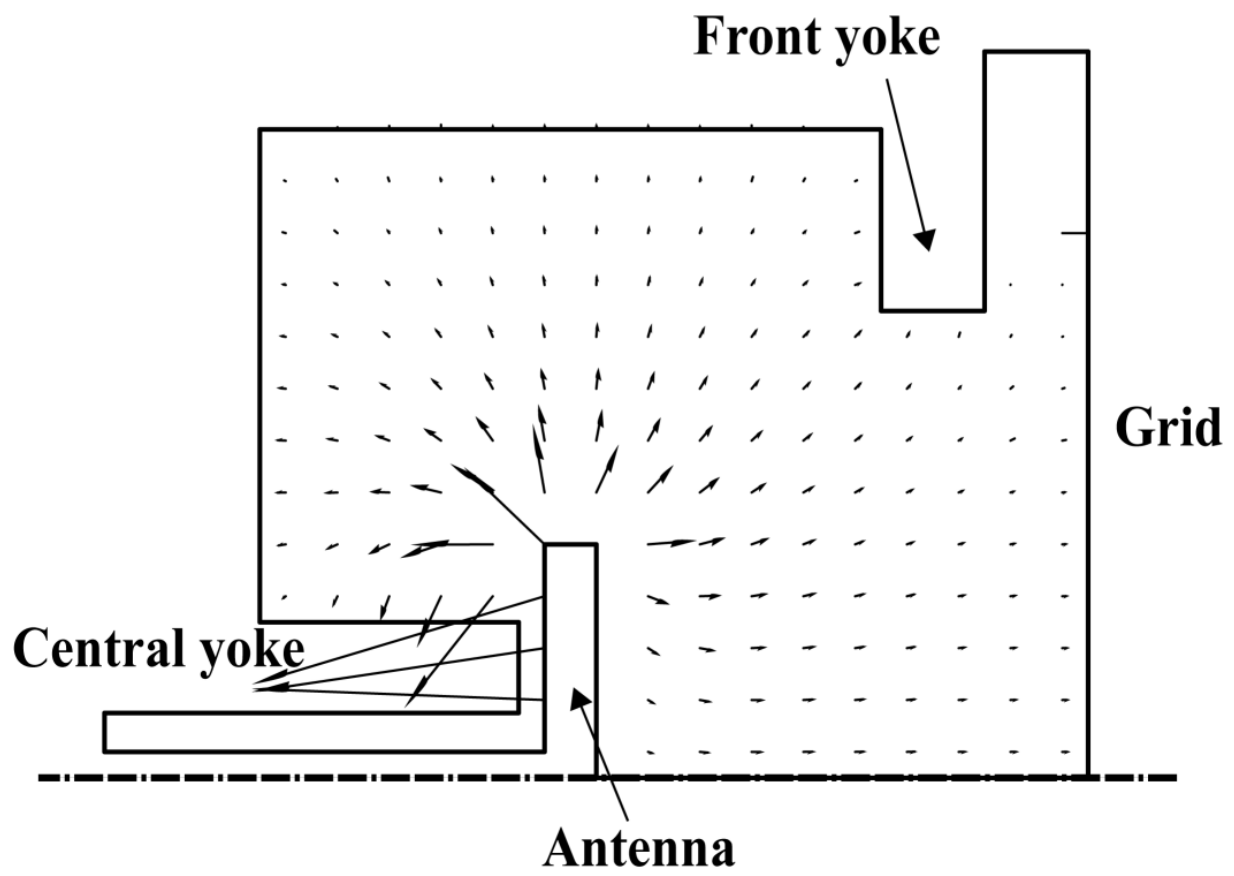
microwave power of 16 W with twelve magnets.

Figure 7. Electric field profile of a miniature microwave discharge ion thruster developed at Kyushu University.
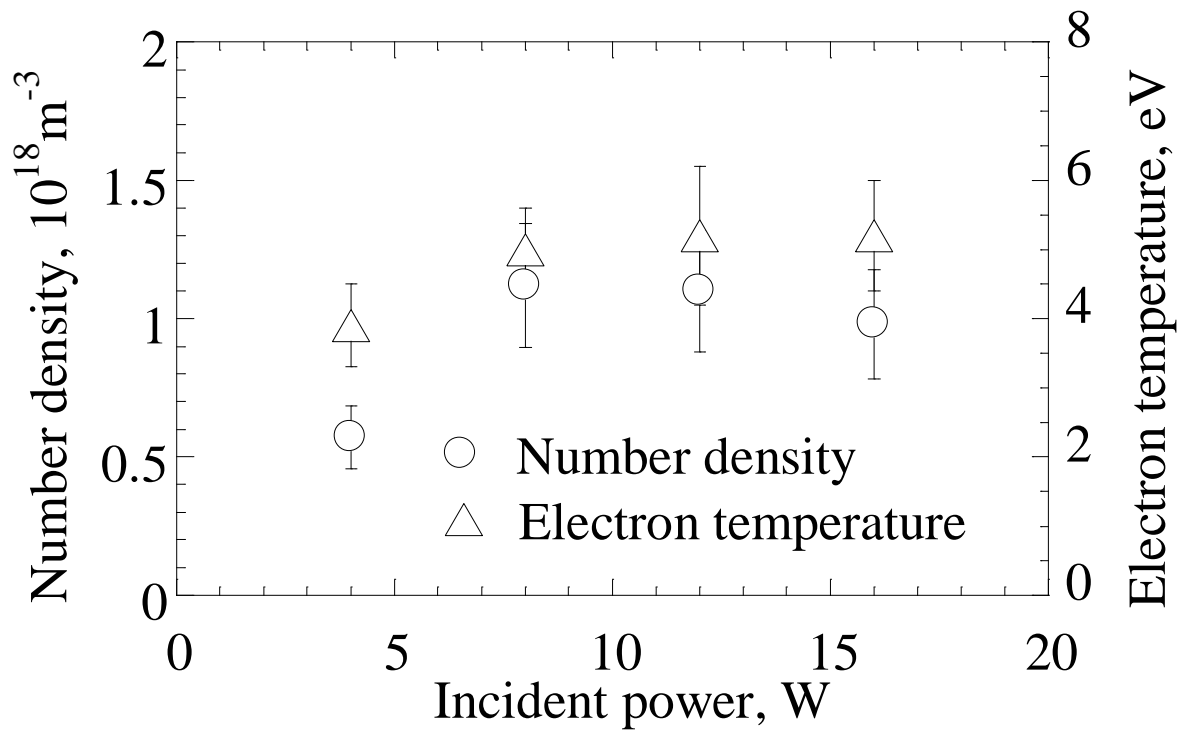
Figure 8. Dependence of plasma properties on incident microwave power at krypton mass flow rate of
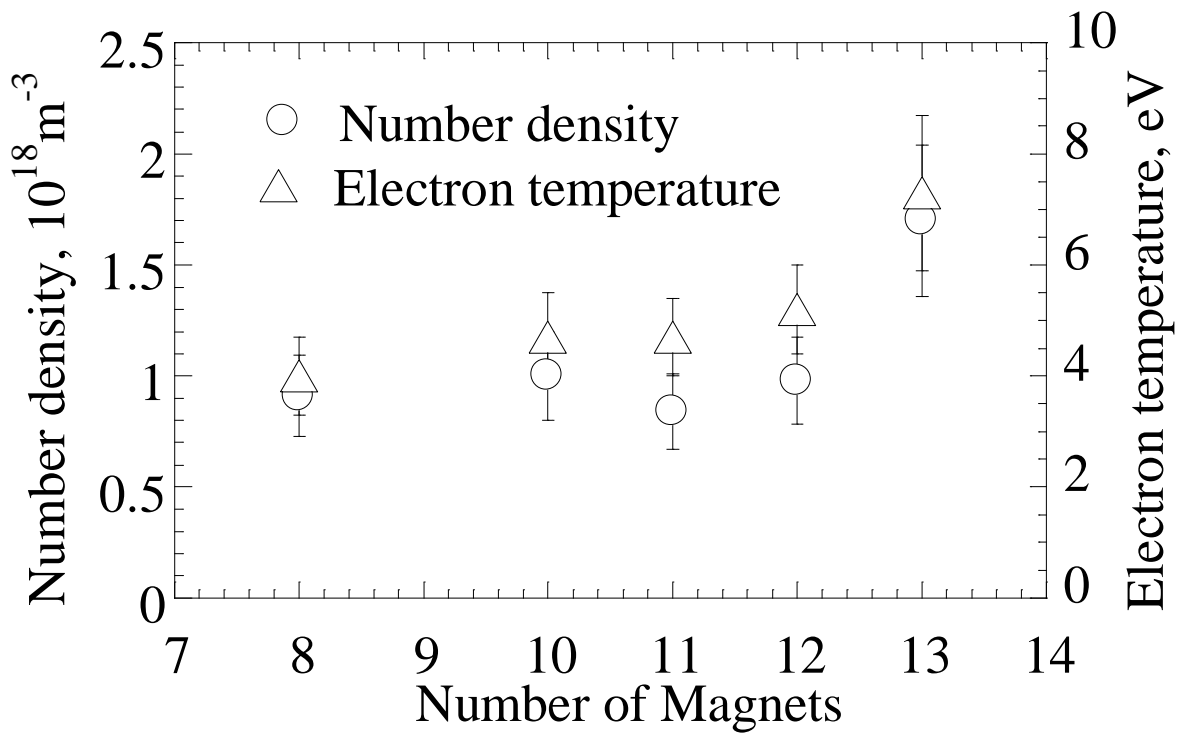
0.025 mg/s, with twelve magnets.

Figure 9. Dependence of plasma properties on the number of magnets at krypton mass flow rate of
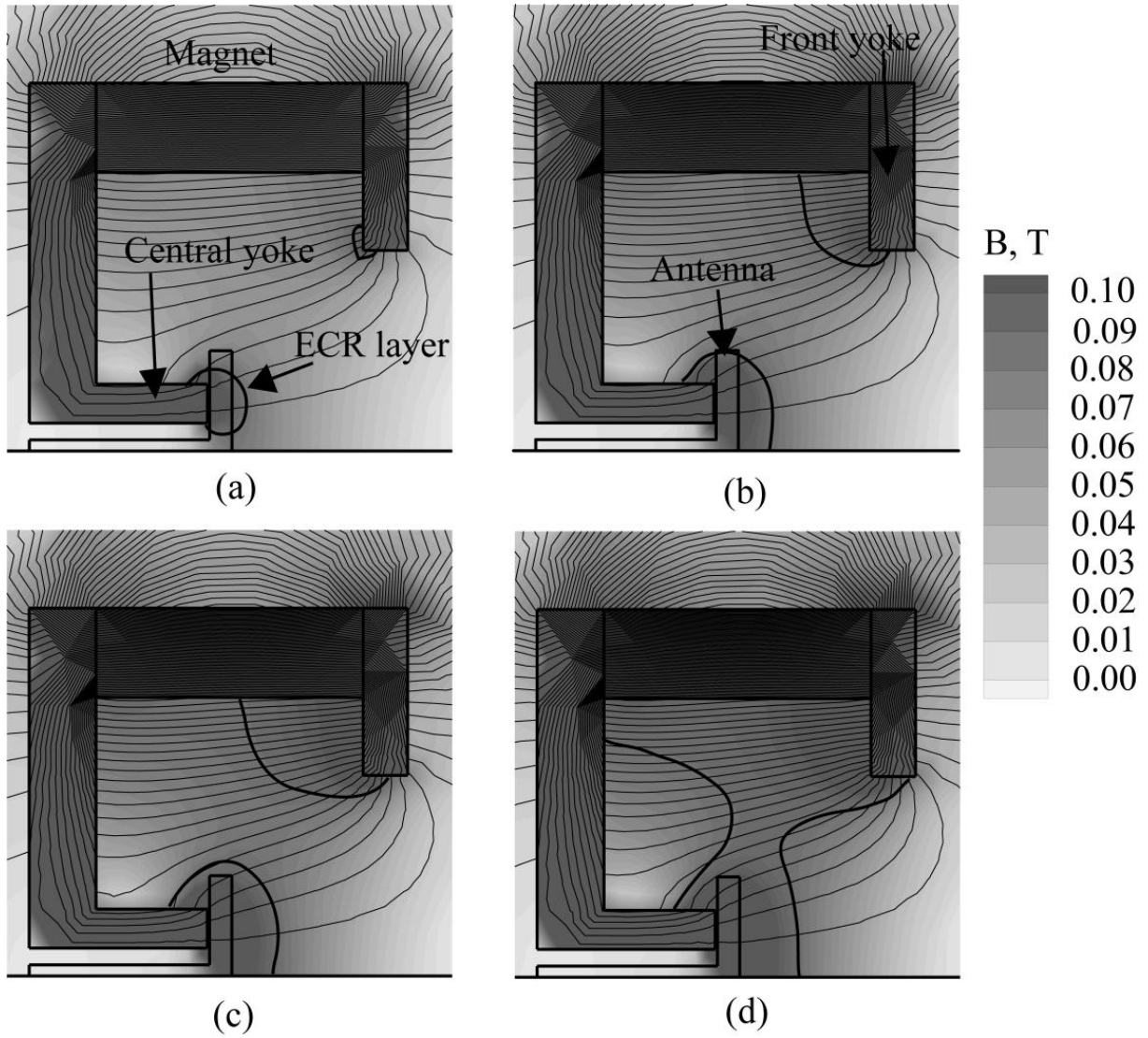
0.025 mg/s and incident microwave power of 16 W.

Figure 10. Magnetic field profile for various numbers of magnets, (a) $N_{mag} = 10$, (b) $N_{mag} = 12$, (c) N_{mag}

$= 13$, (d) $N_{mag} = 14$.